Intraribbon Heterojunction Formation in Ultranarrow Graphene Nanoribbons

Stephan Blankenburg,[†] Jinming Cai,[†] Pascal Ruffieux,[†] Rached Jaafar,[†] Daniele Passerone,[†] Xinliang Feng,[‡] Klaus Müllen,[‡] Roman Fasel,[†,§] and Carlo A. Pignedoli[†,*]

[†]EMPA, Swiss Federal Laboratories for Materials Science and Technology, nanotech@surfaces Laboratory, 8600 Dübendorf, Switzerland, [‡]Max Planck Institute for Polymer Research, Ackermannweg 10, 55124 Mainz, Germany, and [§]Department of Chemistry and Biochemistry, University of Bern, Freiestrasse 3, 3012 Bern, Switzerland

ABSTRACT

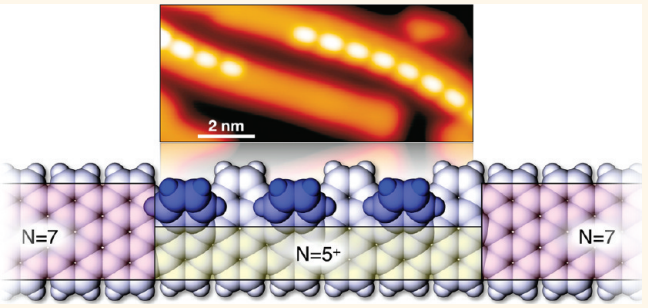

Graphene nanoribbons—semiconducting quasi-one-dimensional graphene structures—have great potential for the realization of novel electronic devices. Recently, graphene nanoribbon heterojunctions—interfaces between nanoribbons with unequal band gaps—have been realized with lithographic etching techniques and *via* chemical routes to exploit quantum transport phenomena. However, standard fabrication techniques are not suitable for ribbons narrower than ~5 nm and do not allow to control the width and edge structure of a specific device with atomic precision. Here, we report the realization of graphene nanoribbon heterojunctions with lateral dimensions below 2 nm *via* controllable dehydrogenation of polyanthrylene oligomers self-assembled on a Au(111) surface from molecular precursors. Atomistic simulations reveal the microscopic mechanisms responsible for intraribbon heterojunction formation. We demonstrate the capability to selectively modify the heterojunctions by activating the dehydrogenation reaction on single units of the nanoribbons by electron injection from the tip of a scanning tunneling microscope.

KEYWORDS: graphene nanoribbon · heterojunction · nanoscale materials · synthesis and processing · molecular self-assembly · computational nanotechnology

Graphene nanoribbons (GNRs) are promising building blocks for novel graphene-based electronic devices.[1] Beyond the most important distinction between zig-zag edge (ZGNR) and armchair edge ribbons (AGNR), more general variations of the geometry of a GNR allow for gap tuning through one-dimensional (1D) quantum confinement. The electronic and optical properties of GNRs as a function of width and topology have been studied by different computational[2−8] and experimental[9,10] approaches. In general, increasing the ribbon width leads to an overall decrease of the band gap, with superimposed oscillation features that are maximized for armchair GNRs (AGNRs).[2−10] More complex geometries, including GNR heterojunctions, have been subject to computational investigation to explore quantum effects such as conductance oscillations, electron lensing, and focusing.[11,12] Recently, graphene nanoribbon heterojunctions have been realized with lithographic etching techniques[11−14] and *via* chemical routes.[15] However, standard fabrication techniques are not suitable for ribbons narrower than ~5 nm and do not allow to control the width and edge structure of a specific device with atomic precision.[16] The strong interest in heterojunctions and heterostructures (combinations of multiple heterojunctions) derives from the fact that they are the fundamental building blocks of modern high-speed- and opto-electronics.[17] Semiconductor heterostructures are usually manufactured by stacking crystalline materials exhibiting different electronic band gaps, which requires the use of molecular beam epitaxy or chemical vapor deposition technologies in order to precisely control the 2D interface. *Lateral* heterojunctions represent an even harder challenge. Polycrystalline graphene allows to exploit (intrinsically lateral) grain boundaries acting as 1D interfaces, and the orientation of confining domain boundaries can be related to the electronic and transport properties, both experimentally and theoretically.[12,18,19] Going from 1D interfaces to "0D" heterojunctions consisting of a finite set of atoms with controlled structure, thus, appears to be a highly appealing next step.

In this respect, intra-GNR heterostructures might provide a completely new concept for the realization of (opto-)electronic devices. Indeed, using GNRs as building

* Address correspondence to carlo.pignedoli@empa.ch.

Received for review August 16, 2011 and accepted February 10, 2012.

Published online February 10, 2012
10.1021/nn203129a

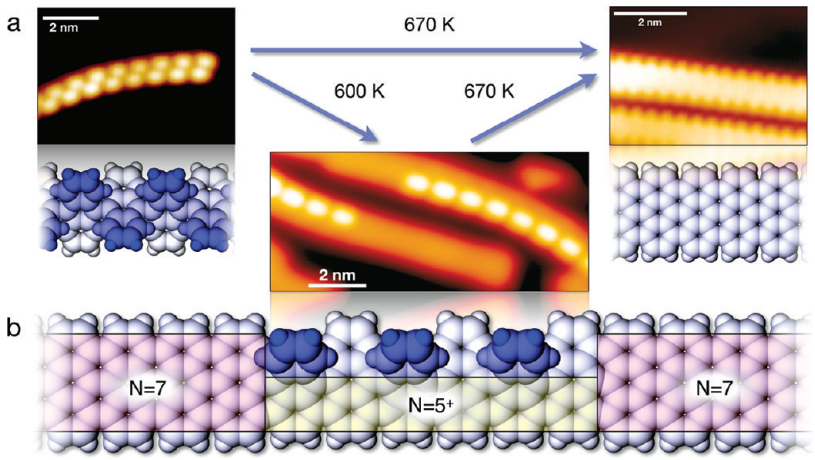

Figure 1. Realization of GNR heterojunctions by partial cyclodehydrogenation of polyanthrylene oligomers. (a) STM measurements and corresponding atomistic models demonstrating the synthesis of AGNRs starting from polyanthrylene chains assembled on a Au(111) substrate. Deposition of the molecular precursor on a substrate held at 470 K results in polyanthrylene oligomers (left) *via* surface-promoted monomer dehalogenation and intermolecular colligation of the resulting biradical intermediates. Annealing at 670 K triggers cyclodehydrogenation resulting in 7-AGNRs (right). (b) Annealing at a reduced temperature of 600 K results in partial cyclodehydrogenation and produces intraribbon heterojunctions. The STM image and the corresponding atomistic model show the realization of an atomically precise junction between a fully reacted $N = 7$ AGNR and a partially reacted polyanthrylene segment ($N = 5^{+}$). STM images are acquired in constant current mode at 35 K ($V_{bias} = 1$ V; $I = 0.1$ nA).

blocks rather than semiconducting crystalline thin films, the unique quantum properties of the constituents can be fully exploited, and the interface between different GNRs can potentially be realized without defects. Band gap tuning between different components of the heterojunction can then simply be achieved by varying the width of the components rather than their chemical composition, potentially allowing for "all-carbon" device components. In this spirit, Prezzi and co-workers computationally characterized ideal AGNR heterojunctions formed by a sequence of ribbons with different width (*e.g.*, $N = 7/8/7$ where N is the number of carbon atom pairs across the ribbon).[20] For the $N = 7/8/7$ heterojunction, "a novel mechanism for the creation of optically active carbon-based QDs with prominent and tunable exciton localization features, which make them suitable for a variety of applications, ranging from single-photon emission to optically-driven quantum information" was demonstrated.[20] Even more recently, Li *et al.*[21] studied the electronic and transport properties of AGNR–ZGNR junctions with *ab initio* methods and called for the corresponding yet-to-come experiments. Because of the inherent limitations of lithographic methods[13,14,10] and of other known approaches to fabricate graphene nanostructures,[16] however, the experimental realization of GNR heterojunctions with the required atomic precision has remained elusive. Bottom-up approaches based on cyclodehydrogenation reactions in solution[22–25] or on solid substrates[26–32] have recently emerged as promising routes to the synthesis of nanoribbons and nanographenes.[32] Here we show that a recently reported bottom-up approach based on metal surface-assisted intermolecular coupling and intramolecular cyclodehydrogenation not only allows for the fabrication of ultranarrow GNRs,[26] but also gives access to GNR heterojunctions with the required atomic precision.

RESULTS AND DISCUSSION

We focus on the key step of this bottom-up GNR fabrication method, which is the surface-assisted thermally induced cyclodehydrogenation of linear polyphenylenes on Au(111) templates (Figure 1a). The method, which does not need a Lewis acid or other catalyst than the supporting metal substrate, is highly selective and efficient, but nothing is known about the details of this unique reaction. We consider the particular case of the polyanthrylene polymer transforming into $N = 7$ AGNRs (7-AGNR). Scanning tunneling microscopy (STM) experiments demonstrate that polyanthrylene chains adsorbed on Au(111) substrates (Figure 1a) undergo cyclodehydrogenation upon annealing at 670 K: the ends of the anthryl units alternately pointing "up" and "down" couple with each other and transform the buckled polymer chain into a fully planar 7-AGNR (Figure 1a). To understand the microscopic details of this reaction, we employed state-of-the-art atomistic simulations based on density functional theory (DFT) for a model system mimicking an infinite polyanthrylene chain adsorbed on a Ag(111) surface (see Methods section and Supporting Information for details). The calculations reveal a fundamental feature in the dehydrogenation process of the polymer chain: neighboring units on the *same* side of the polymer axis react like in a domino effect, until one side is fully cyclodehydrogenated, while the other still exhibits the original, uncoupled up-and-down units

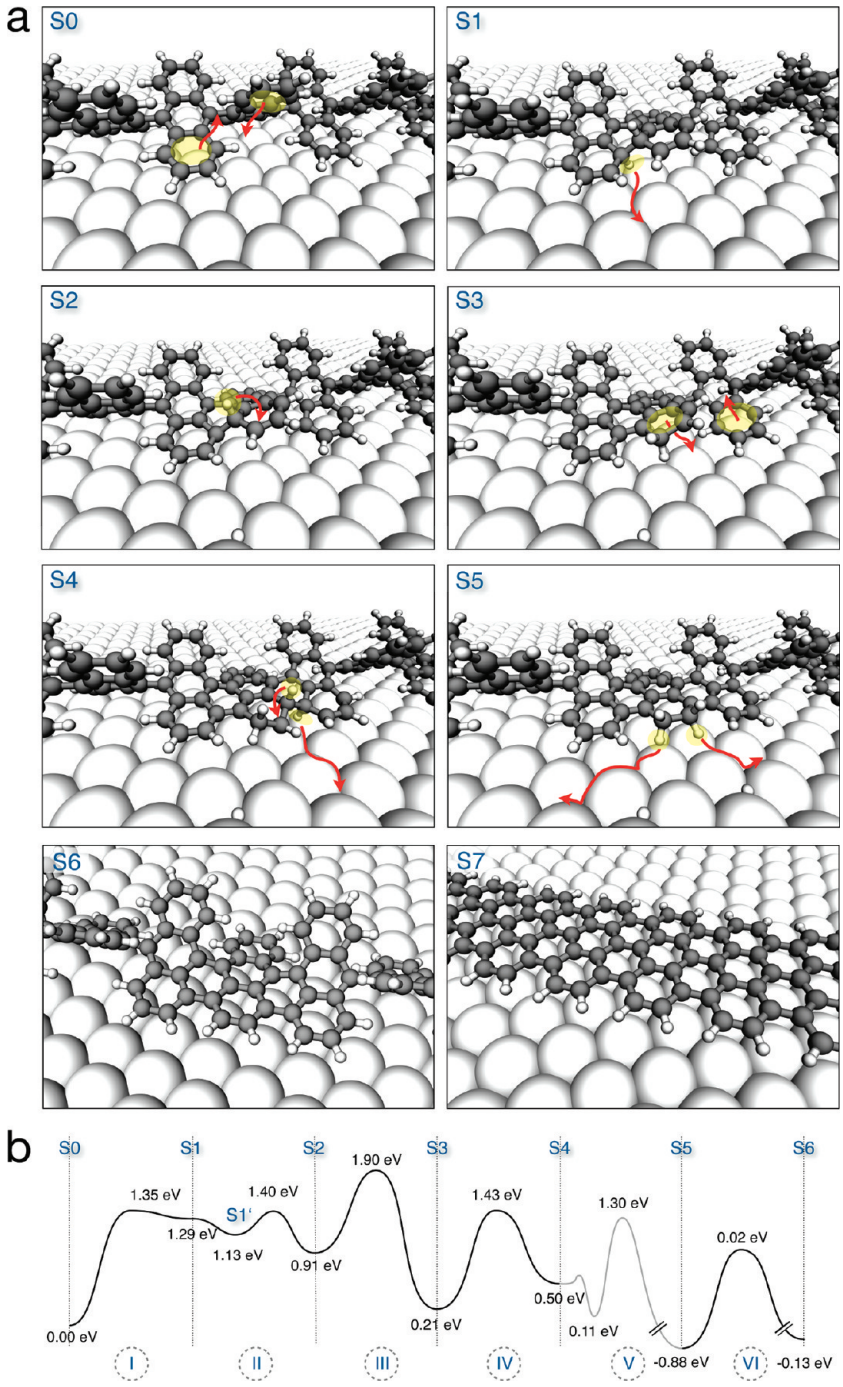

Figure 2. Mechanism of the cyclodehydrogenation reaction as revealed by DFT calculations. (a) Atomic models representing the geometries of the intermediate states along the reaction path. Large white spheres represent silver atoms of the Ag(111) substrate. The three up−down repetition units of the polymer included in the simulation cell are visible. Small gray/white spheres represent the carbon/hydrogen atoms of the molecular structure. Arrows indicate atomic rearrangements that will occur in the highlighted regions upon the transition from one geometry to the next . (b) Energy diagram of the elementary steps that, iterated, transform the unreacted polyanthrylene chain S0 to the 7-AGNR S7. The energies of the intermediate metastable configurations and of the transition state configurations are given relative to the initial configuration S0. The line is a guide to the eye. The gray line between S4 and S5 indicates that this step is a combination of several processes; only the highest barrier is indicated.

(Figure 1b). This unanticipated cyclodehydrogenation sequence suggests that careful control of annealing temperature and duration might allow to obtain partially reacted AGNR segments. In fact, 5 min of annealing at 600 K produces partially cyclodehydrogenated ribbons (Figure 1b). These ribbons consist of segments exhibiting the 7-AGNR structure and of one-side-only dehydrogenated segments. The latter can be viewed as $N = 5$ AGNRs with additional benzene rings *ortho*-fused to the naphthalene units (5^{+}-AGNR). Standard

DFT calculations of the electronic properties of the partially dehydrogenated 5^+-AGNRs and of the 7-AGNR (see Supporting Information) reveal a band gap difference of 0.3 eV. GNRs consisting of alternating $N = 7$ and $N = 5^+$ segments, as shown in Figure 1b, thus, provide a first realization of intraribbon heterostructures, with properties potentially very similar to the ones predicted by Prezzi and co-workers.[20]

To understand the unanticipated evolution of the dehydrogenation, we follow the atomistic details of the reaction with reference to Figure 2. The reaction is driven by the van der Waals (vdW) metal/polymer attraction that energetically favors flat conformations of the polymer chain, and by covalent interactions with the substrate that stabilize radical intermediates (see Supporting Information). We simulate an infinite chain by means of three molecular units (= six anthryles) with periodic boundary conditions. The full cyclodehydrogenation is obtained by iterating a reaction sequence consisting of six elementary steps involving one and a half molecular units: two "down" (toward the surface) and one "up" pointing anthryl ends on one side of the polymer axis (see Figure 2a).

In *step I*, due to vdW interactions with the substrate, the polymer flattens with respect to its ideal geometry in vacuum, facilitating the formation of a C–C bond between two consecutive "up" and "down" units. In this process, one of the H atoms is pushed away from the surface, while the other points toward the substrate. In *step II*, the latter H atom is catalytically detached, binds to the metal surface, and migrates away from the polymer. Covalent binding to the substrate (see Supporting Information) stabilizes the resulting radical carbon. In *step III*, the hydrogen atom that was pointing outward shifts to the neighboring carbon atom at the edge of the polymer, thus, forming a local CH_2 termination. This further increases planarity and is also driven by vdW interactions. The following steps are essentially repetitions of the previous ones albeit with modified activation energies as revealed by Figure 2b. We find that the reaction, rather than continuing on the opposite side of the polymer axis like in a zippering mechanism, actually continues on the *same* side ("one-side domino") due to the established flattening that lowers the latter activation barrier with respect to the one on the opposite side. Cyclodehydrogenation thus continues on one-side only, with another C–C bond being formed and the corresponding out- and inward C–H bending (*step IV*), followed again by surface-catalyzed H detachment and an outward H-shift (step V), which results in a fully flattened down-up-down unit (S5). Finally, *step VI* corresponds to a further dehydrogenation where the CH_2 termination resulting from steps III and V is reduced to a CH termination.

These six steps could now be iterated again, either on the opposite side of the chain, or along the same side in the neighboring up-down-up unit. Because of the reduced flexibility of the partially reacted chain, continuation of the reaction on the same side is clearly favored (see also Supporting Information). This gives rise to the unanticipated "one-side-domino" cyclodehydrogenation sequence: the neighboring units on the *same* side of the polymer axis react like in a falling row of dominoes, until one side is fully coupled while the other still exhibits the original, uncoupled up-and-down units. This allows us to realize heterojunctions by annealing at a reduced temperature (Figure 1b).

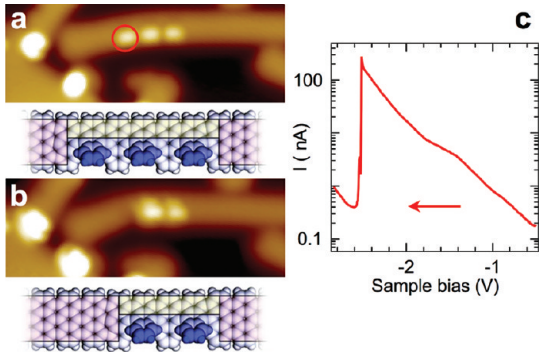

Figure 3. Tip-induced cyclodehydrogenation. (a) STM image and corresponding atomistic model of a $N = 7/5^+/7$ heterojunction obtained *via* controlled annealing.; (b) STM image and corresponding atomistic model of the previous heterojunction after tip-induced dehydrogenation of one additional unit; (c) $I-V$ curve taken at the position marked in panel a, revealing the activation of the reaction at −2.5 V. The tip height is stabilized using $V_{bias} = 1.0$ V and $I = 0.1$ nA. During $I-V$ data acquisition, the feedback loop is turned off.

Evidently, the fabrication of 7-AGNR/5^+-AGNR heterojunctions *via* moderate annealing does not provide sufficient control on the length and position of either GNR segments. Technologically more appealing procedures for the fabrication of this particular kind of GNR heterojunctions would certainly need to rely on light- or electron-stimulated[33,34] cyclodehydrogenation that should allow to lithographically imprint a desired sequence of partially and fully cyclodehydrogenated segments into the polymer. As a first step along these lines, we have verified that cyclodehydrogenation can indeed be triggered by electron injection from the tip of an STM. Starting from heterojunctions obtained as outlined above *via* moderate annealing, we demonstrate the ability to shorten the length of 5^+-AGNR regions in favor of 7-AGNR segments by controlled cyclodehydrogenation using voltage pulses applied to the STM tip. Figure 3 shows an example of a 7-GNR with a 5^+-AGNR region, where the 5^+-AGNR region is shortened by one unit *via* electron activated dehydrogenation. Experimentally, the tip is placed at the indicated location (Figure 3a) and stabilized in height using the indicated tunneling parameters. The voltage ramp is then performed with open feedback loop, that is, at constant height. We find that dehydrogenation is favorably triggered when tunneling into

the occupied states of polyanthryl below ~2 V. Typical critical parameters are −2.5 V and tunneling currents of ~200 nA. The marked increase of the tunneling current during the voltage ramp (Figure 3c) is related to the need of large negative bias values and the related tunneling transmission that increases with the magnitude of the applied sample bias.[35] Furthermore, we find that tips allowing for electron-induced cyclodehydrogenation show an increased sensitivity to occupied polyanthryl states, presumably related to a pronounced overlap of the occupied polyanthryl and electronic states of the tip.

CONCLUSIONS

We have fabricated intraribbon GNR heterojunctions *via* temperature induced partial cyclodehydrogenation of a surface-anchored polyanthrylene chain. Importantly, the details of the cyclodehydrogenation pathway have been unraveled by extensive *ab initio* calculations, which reveal why the process does not need the presence of a Lewis acid or other catalysts and makes it possible to synthesize GNRs and heterojunctions under vacuum conditions. We have finally shown that cyclodehydrogenation may also be induced locally by electron injection from the tip of a STM, which suggests that GNR heterostructure imprinting might become feasible using electron beam "writing". Our results demonstrate the power of bottom-up approaches for the fabrication of graphene-based nanostructures showing great promise for electronic applications. The necessary next step toward all-graphene based architectures for (opto) electronic devices is a reliable transfer of the graphene nanostructures fabricated on metal templates onto semiconducting substrates. Experiments along these lines are under way and indicate that clean, efficient and nondestructive transfer is indeed feasible [Pang, S.; Cai, J.; Feng, X.; Müllen, K.; Ruffieux, P.; Fasel, R., unpublished results].

METHODS

STM Experiments. The molecular precursor 10,10′-dibromo-9,9′-bianthryl was sublimated at a rate of 1 Å/min for 100 s onto a clean Au(111) single crystal substrate (Surface Preparation Laboratory, The Netherlands) which was cleaned by repeated cycles of argon ion bombardment and annealing to 750 K. The substrate was maintained at 470 K during deposition to induce dehalogenation and radical addition. Then, the sample was postannealed at 600 K for 5 min to partially cyclodehydrogenate the polymers, or at 670 K to fully cyclodehydrogenate the polymer. A variable-temperature STM and a low-temperature STM, both from Omicron Nanotechnology, were used to characterize the morphology and induce the dehydrogenation of the GNRs. STM images and STS data were taken in the constant current mode under ultra-high-vacuum conditions at sample temperatures of 35 K in the variable temperature STM and 5 K in the low-temperature STM.

Atomistic Simulations. Our simulations are based on large-scale *ab initio* calculations[36] where the whole system, adsorbate and substrate, is treated within density functional theory that allows to describe properly the catalytic contributions from the substrate to the reaction. To account for the influence of the van der Waals interaction between the polymer and the substrate, we used a semi-empirical scheme in the form of C_6/R^6 proposed by Grimme.[37] Since initial experiments done on Ag(111) indicated an identical polyanthrylene cyclodehydrogenation behavior than on Au(111), modeling of the polyanthrylene cyclodehydrogenation was done on a Ag(111) rather than the Au(111) surface to avoid complications arising from the herringbone reconstruction of Au(111). The polyanthrylene/metal surface system is modeled by periodically repeated slabs[38] with a lateral size of ~22 × 26 Å^2, containing the silver atoms of the substrate, the adsorbed polymer and a vacuum region 20 Å thick. The energy of the different intermediate states was computed optimizing the corresponding geometries and the transition states connecting consecutive intermediates were identified by the climbing image nudged elastic band method.[39]

To model the reaction in an unbiased way—under the hypothesis of an infinite chain (contrary to ref 31 where very short chain segments were considered)—one needs a minimum of three precursor units due to the commensurability of the polymer and the silver substrate as well as for the description of an uncorrelated cyclodehydrogenation sequence. In our model, we included three molecular units.

Conflict of Interest: The authors declare no competing financial interest.

Acknowledgment. Extensive calculations were enabled by grants of the Swiss National Supercomputing Centre (CSCS) in Manno, and of the Swiss National Science Foundation (R'Equip UP-IPAZIA). The Alexander von Humboldt Foundation, the Swiss National Science Foundation and the NCCR Nanoscale Science are acknowledged for financial support. This work has been supported by the European Science Foundation (ESF) under the EUROCORES Programme EuroGRAPHENE (GOSPEL).

Supporting Information Available: Experimental and computational details, details of the cyclodehydrogenation pathway (including movie), alternative reaction pathway, band structures, additional STM images of GNR heterojunctions and tip-induced local cyclodehydrogenation. This material is available free of charge *via* the Internet at http://pubs.acs.org.

REFERENCES AND NOTES

1. Dutta, S.; Pati, S. K. Novel Properties of Graphene Nanoribbons: A Review. *J. Mater. Chem.* **2010**, *20*, 8207–8223.
2. Ezawa, M. Peculiar Width Dependence of the Electronic Properties of Carbon Nanoribbons. *Phys. Rev. B* **2006**, *73*, 045432.
3. Yang, L.; Park, C.-H.; Son, Y.-W.; Cohen, M. L.; Louie, S. G. Quasiparticle Energies and Band Gaps in Graphene Nanoribbons. *Phys. Rev. Lett.* **2007**, *99*, 186801.
4. Son, Y.-W.; Cohen, M. L.; Louie, S. G. Energy Gaps in Graphene Nanoribbons. *Phys. Rev. Lett.* **2006**, *97*, 216803.
5. Son, Y.-W.; Cohen, M. L.; Louie, S. G. Half Metallic Graphene Nanoribbons. *Nature* **2006**, *444*, 347–349.
6. Nakada, K.; Fujita, M.; Dresselhaus, G.; Dresselhaus, M. S. Edge State in Graphene Nanoribbons: Nanometer Size Effect and Edge Shape Dependence. *Phys. Rev. B* **1996**, *54*, 17954–17961.
7. Barone, V.; Hod, O.; Scuseria, G. E. Electronic Structure and Stability of Semiconducting Graphene Nanoribbons. *Nano Lett.* **2006**, *6*, 2748–2754.
8. Prezzi, D.; Varsano, D.; Ruini, A.; Marini, A.; Molinari, E. Optical Properties of Graphene Nanoribbons: The Role of Many-Body Effects. *Phys. Rev. B* **2008**, *77*, 041404.
9. Shimizu, T.; Haruyama, J.; Marcano, D. C.; Kosinkin, D. V.; Tour, J. M.; Hirose, K.; Suenaga, K. Large Intrinsic Energy Bangaps in Annealed Nanotube-Derived Graphene Nanoribbons. *Nat. Nanotechnol.* **2011**, *6*, 45–50.

10. Han, M. Y.; Özyilmaz, B.; Zhang, Y.; Kim, P. Energy Band-Gap Engineering of Graphene Nanoribbons. *Phys. Rev. Lett.* **2007**, *98*, 206805.
11. Kim, P.; Han, M. Y.; Young, A. F.; Meric, I.; Shepard, K. L. Graphene Nanoribbon Devices and Quantum Heterojunction Devices. *IEEE Int. Electron Devices Meet.* **2009**, 241–244.
12. Young, A. F.; Kim, P. Quantum Interference and Klein Tunneling in Graphene Heterojunctions. *Nat. Phys.* **2009**, *5*, 222–226.
13. Ponomarenko, L. A.; Schedin, F.; Katsnelson, M. I.; Yang, R.; Hill, E. W.; Novoselov, K. S.; Geim, A. K. Chaotic Dirac Billard in Graphene Quantum Dots. *Science* **2008**, *320*, 356–358.
14. Chen, Z.; Lin, Y.-M.; Rooks, M. J.; Avouris, P. Graphene Nano-Ribbon Electronics. *Phys. E* **2007**, *40*, 228–232.
15. Li, X.; Wang, X.; Zhang, L.; Lee, S.; Dai, H. Chemically Derived, Ultrasmooth Graphene Nanoribbon Semiconductors. *Science* **2008**, *319*, 1229–1232.
16. Wei, D.; Liu, Y. Controllable Synthesis of Graphene and its Applications. *Adv. Mater.* **2010**, *22*, 3225–3241.
17. Franciosi, A.; Van de Walle, C. G. Heterojunction Band Offset Engineering. *Surf. Sci. Rep.* **1996**, *25*, 1–140.
18. Lahiri, J.; Lin, Y.; Boskurt, P.; Oleynik, I. I.; Batzill, M. An Extended Defect in Graphene as a Metallic Wire. *Nat. Nanotechnol.* **2010**, *5*, 326–329.
19. Yazyev, O.; Louie, S. Electronic Transport in Polycrystalline Graphene. *Nat. Mater.* **2010**, *9*, 806–809.
20. Prezzi, D.; Varsano, D.; Ruini, A.; Molinari, E. Quantum-Dot States and Optical Excitations in Edge-Modulated Graphene Nanoribbons. *Phys. Rev. B* **2011**, *84*, 041401(R).
21. Li, X.-F.; Wang, L.-L.; Chen, K.-Q.; Luo, Y. Design of Graphene-Nanoribbon Heterojunctions from First Principles. *J. Phys. Chem. C* **2011**, *115*, 12616–12624.
22. Yang, X.; Dou, X.; Rouhanipour, A.; Zhi, L.; Räder, H. J.; Müllen, K. Two-Dimensional Graphene Nanoribbons. *J. Am. Chem. Soc.* **2008**, *130*, 4216–4217.
23. Dössel, L.; Gherghel, L.; Feng, X.; Müllen, K. Graphene Nanoribbons by Chemists: Nanometer-Sized, Soluble, and Defect-Free. *Angew. Chem., Int. Ed.* **2011**, *50*, 2540–2543.
24. Fogel, Y.; Zhi, L.; Rouhanipour, A.; Andrienko, D.; Räder, H. J.; Müllen, K. Graphitic Nanoribbons with Dibenzo[e, l]pyrene Repeat Units: Synthesis and Self-Assembly. *Macromolecules* **2009**, *42*, 6878–6884.
25. Wu, J.; Gherghel, L.; Watson, M. D.; Li, J.; Wang, Z.; Simpson, C. D.; Kolb, U.; Müllen, K. From Branched Polyphenylenes to Graphite Ribbons. *Macromolecules* **2003**, *36*, 7082.
26. Cai, J.; Ruffieux, P.; Jaafar, R.; Bieri, M.; Braun, T.; Blankenburg, S.; Muoth, M.; Seitsonen, A. P.; Moussa, S.; Feng, X.; et al. Atomically Precise Bottom-Up Fabrication of Graphene Nanoribbons. *Nature* **2010**, *466*, 470–473.
27. Weiss, K.; Beernink, G.; Dötz, F.; Birkner, A.; Müllen, K.; Wöll, C. H. Template-Mediated Synthesis of Polycyclic Aromatic Hydrocarbons: Cyclodehydrogenation and Planarization of a Hexaphenylbenzene Derivative at a Copper Surface. *Angew. Chem., Int. Ed.* **1999**, *38*, 3748–3752.
28. Rim, K. T.; Siaj, M.; Xiao, S.; Myers, M.; Carpentier, V. D.; Liu, L.; Su, M.; Steigerwald, M. L.; Hybersten, M. S.; McBreen, P. H.; et al. Forming Aromatic Hemispheres on Transition-Metal Surfaces. *Angew. Chem., Int. Ed.* **2007**, *46*, 7891–7895.
29. Otero, G.; Biddau, G.; Sánchez-Sánchez, C.; Caillard, R.; López, M. F.; Rogero, C.; Palomares, F. J.; Cabello, N.; Basanta, M. A.; Ortega, J.; et al. Fullerenes from Aromatic Precursors by Surface-Catalysed Cyclodehydrogenation. *Nature* **2008**, *454*, 865–868.
30. Treier, M.; Pignedoli, C. A.; Laino, T.; Rieger, R.; Müllen, K.; Passerone, D.; Fasel, R. Surface-Assisted Cyclodehydrogenation Provides a Synthetic Route towards Easily Processable and Chemically Tailored Nanographenes. *Nat. Chem.* **2011**, *3*, 61–67.
31. Björk, J.; Stafström, S.; Hanke, F. Zipping Up: Cooperativity Drives the Synthesis of Graphene Nanoribbons. *J. Am. Chem. Soc.* **2011**, *133*, 14884–14887.
32. Wu, J. S.; Pisula, W.; Müllen, K. Graphenes as Potential Material for Electronics. *Chem. Rev.* **2007**, *107*, 718–747.
33. Mirua, A.; De Feyter, S.; Abdel-Mottaleb, M. M. S.; Gesquière, A.; Grim, P. G. M.; Moessner, G.; Sieffert, M.; Klapper, M.; Müllen, K.; De Schryver, F. C. Light-and STM-Tip-Induced Formation of One-Dimensional and Two-Dimensional Organic Nanostructures. *Langmuir* **2003**, *19*, 6474–6482.
34. Okawa, Y.; Aono, M. Materials Science: Nanoscale Control of Chain Polymerization. *Nature* **2001**, *409*, 683–684.
35. Buchs, G; Ruffieux, P.; Gröning, P.; Gröning, O. Defect-Induced Negative Differential Resistance in Single-Walled Carbon Nanotubes. *Appl. Phys. Lett.* **2008**, *93*, 73115.
36. VandeVondele, J.; Krack, M.; Mohamed, F.; Parrinello, M.; Chassaing, T.; Hutter, J. Quickstep: Fast and Accurate Density Functional Calculations Using a Mixed Gaussian and Plane Waves Approach. *Comput. Phys. Commun.* **2005**, *167*, 103–128. http://cp2k.berlios.de.
37. Grimme, S. Semiempirical GGA-Type Density Functional Constructed With a Long-Range Dispersion Correction. *J. Comput. Chem.* **2006**, *27*, 1787–1799.
38. Pickett, W. E. Pseudopotential Methods in Condensed Matter Applications. *Comp. Phys. Rep.* **1989**, *9*, 115–198.
39. Henkelman, G.; Uberuaga, B. P.; Jonsson, H. A. Climbing Image Nudged Elastic Band Method for Finding Saddle Points and Minimum Energy Paths. *J. Chem. Phys.* **2000**, *113*, 9901.